Talanta 233 (2021) 122580

Contents lists available at ScienceDirect

Talanta

journal homepage: www.elsevier.com/locate/talanta

Development of a miniature protein mass spectrometer capable of analyzing native proteins

Qian Xu, Jie Hong, Siyu Liu, Yanbing Zhai, Wei Xu *

School of Life Science, Beijing Institute of Technology, Beijing, 100081, China

ARTICLE INFO

Keywords:
Miniature mass spectrometer
Linear ion trap
Native protein
Protein conformation

ABSTRACT

Current miniature mass spectrometers were usually designed for the detection of small and medium size molecules, including volatile (semi-volatile) compounds, drugs and lipids. In this study, a miniature protein mass spectrometer was developed in this work, which could serve as a biosensor for the rapid identification of proteins as well as their conformations. A linear ion trap with a field radius of 2.5 mm was designed to extend mass range of the instrument to over 6500 Th. Mass resolution and sensitivity of the instrument were also optimized for protein ions by increasing the buffer gas pressure and using a high-gain Faraday detector. It is then demonstrated that the mass spectra of native proteins, such as IgG1, could be acquired by coupling the instrument with a soft electrospray ionization source. As a proof-of-concept demonstration, results suggest that the current instrument could be used to identify target proteins and probe/distinguish their conformations in solutions.

1. Introduction

Mass spectrometry (MS) is a powerful analytical technique, which has been widely used for the analyses of volatile [1–5], semi-volatile [6–8] and nonvolatile samples [4,9–13]. Conventional lab-scale mass spectrometers possess high analytical performances, but they also suffer from inconvenience in terms of size, power consumption and complicated operation. The development of miniature mass spectrometer could date back to the 1960s [14], in which a "briefcase" mass spectrometer was built for NASA to measure the Martian atmosphere. Since then, many miniature mass spectrometers have been built for different outer space exploration missions [15]. Atmosphere component, water and small organic molecules are the major targets of these mass spectrometers [16–19]. With increasing demands in national security and environmental protection around year 2000, miniature/portable mass spectrometers were developed and applied in these fields to monitor chemical warfare agents (CWA), explosives and volatile organic compounds (VOC) [20–24]. Since volatile or semi-volatile samples are analyzed, some instruments miniaturization was realized by eliminating Turbo pumps, which resulted in a significant reduction in MS system size, weight, and power [25–27]; while some instruments miniaturization was realized by adopting membrane inlet or low conductance gas inlet designs [15,28].

For non-volatile samples, analyte molecules are typically desorbed and ionized by ionization sources in the atmosphere, and an atmospheric pressure interface is required to efficiently transfer ions to mass analyzers in vacuum [29,30]. In 2008, a miniature mass spectrometer equipped with the discontinuous atmospheric pressure interface (DAPI) was proposed by Purdue University [31]. DAPI breaks the pumping barrier of a miniature mass spectrometer, and enables the coupling of atmospheric pressure ionization sources with a miniature mass spectrometer for non-volatile sample analyses. To improve system duty cycle and robustness, a continuous atmospheric pressure interface (CAPI) was later developed in 2015 [32]. After that, several generations of miniature mass spectrometers have been built with improved analytical performances [33–35]. With a mass range typically below 2000 Th, these instruments have been applied for the analyses of small organic molecules, such as drugs and lipids [4,36,37].

Currently, the analyses of large biomolecules, proteins from instance, are usually performed on lab-scale mass spectrometers. Two major approaches, bottom-up and top-down proteomics, are widely used for protein analyses [38,39]. However, protein molecules have relatively large molecular weights and complex tertiary structures, and it is still challenging to obtain protein sequence and structure information accurately [40]. Up to now, various techniques have been proposed to better analyze protein molecules and protein complexes [41]. For

* Corresponding author. School of Life Science, Beijing Institute of Technology, Haidian, Beijing, 100081, China.
E-mail address: weixu@bit.edu.cn (W. Xu).
URL: https://www.labxing.com/msgroup (W. Xu).

https://doi.org/10.1016/j.talanta.2021.122580
Received 27 April 2021; Received in revised form 27 May 2021; Accepted 28 May 2021
Available online 1 June 2021

instance, techniques including H/D exchange, chemical cross-linking, covalent labeling, native MS, ion mobility spectrometry (IMS) and mobility capillary electrophoresis (MCE) have been developed and used together with high performance mass spectrometers to study protein high-order structures [42–49]. On the other hand, efforts have also been made to extend the mass range and resolution of a mass spectrometer for large protein ion analyses. Time of flight (TOF) and Orbitrap based mass spectrometers with extended mass ranges have been optimized for protein exploration [26,40,41,50]. Charge detection mass spectrometers (CDMS) and digital ion trap based compact mass spectrometers have also been developed [51–55]. For example, Wen-ping Peng et al. measured the cell and microparticle mass distribution by the CDMS [56]. In 2019, Zongxiu Nie et al. adopted a 3D quadrupole ion trap and a charge detector to form a miniature particle mass spectrometer which could measure polystyrene spheres, silica particles, and mice red blood cells [51]. Chung-Hsuan Chen et al. expanded the mass range of a QIT and combined with MALDI and ESI technologies, and they realized single-charge detection of biological macromolecules such as IgG and IgA [57]. These studies adopted QIT as the mass analyzer, and the aim of these mass spectrometers is to detect the mass of larger particle or biological molecules instead of their native conformations.

As a continuous effort to further extend the range of samples that a miniature mass spectrometer could study, an ion trap based miniature protein mass spectrometer was constructed and characterized in this work. Mass range of the instrument was extended from 2000 to over 6500 Th. A relatively high buffer gas pressure in the ion trap was used, so that optimized mass resolution and detection sensitivity could be achieved for protein ions. The performance of a conventional electron multiplier (EM) and a home-built Faraday detector was also compared. After optimization, the instrument was used to perform native MS analysis of five intact proteins. The mass to charge (m/z) ratio and charge state distribution obtained from this instrument could help the rapid screening of target proteins and estimating their conformations.

2. Experimental section

2.1. Sample preparation

Peptide mrfa (MW 524), angiotensin II (MW 1046.18) and proteins including insulin, cytochrome C, lysozyme, bovine serum albumin (BSA) were purchased from Sigma Aldrich (St. Louis, MO, USA). Trastuzumab is a humanized IgG1 monoclonal antibody, which was purchased from Roche Pharama (Schweiz) Ltd. (Basel, Switzerland). Ammonium acetate (CH_3COONH_4) and formic acid (FA) were purchased from Aldrich Chemical Co. (Milwaukee, WI). Deionized water used in this work was purchased from Wahaha company (Hangzhou, China).

The above chemicals were used for the preparation of samples and buffers. In this work, there were two kinds of buffers: deionized water and 20 mmol L^{-1} ammonium acetate solution. Peptide angiotensin II was diluted in deionized water. All protein samples and Trastuzumab were diluted in the ammonium acetate buffer. All experiments were completed in a laboratory with a room temperature.

2.2. Instrumentation

A home developed miniature mass spectrometer was modified to carry out experiments in this work. Fig. 1a is the structure diagram of the miniature protein mass spectrometer. Details about the general instrument setup can also be found in our previous publications [32]. A nano-electrospray ionization (nanoESI) source was used to generate ions. The flow rate of the sample is set at 1 μL min^{-1}. A 3000 V DC voltage was applied on the nanoESI emitter. Inlet of the mass spectrometer was heated to a temperature of ~180 °C to help the desolvation process. The ion transmission part of the miniature mass spectrometer consists of a capillary, an ion funnel, a skimmer and a set of Einzel lens. Based on our existing control circuit, we reduced the field radius of the liner ion trap (LIT) from 4 to 2.5 mm to expand the mass range of the instrument. The LIT (2.5 × 2.5 × 40 mm) placed in the second vacuum stage has hyperbolic electrodes in x-y directions. A voltage scanning RF signal (930–520 kHz) was applied to drive the LIT, and dipolar resonance ejection was applied to mass electively eject ions. Frequency of the dipolar resonance ejection AC signal was set at ~1/3 of the RF frequency, otherwise specified. The 3D component assembly of the mini protein mass spectrometer system could be found in in Fig. 1b. The overall size of the mini mass spectrometer is about 20 × 35 × 31 cm. The instrument was 22 kg in weight, and power-supplied by an adapter with a power consumption of 300 W in total.

During the operation of an ion trap, buffer gas would play important roles during the ion injection, cooling and ejection steps. Since protein ions are much heavier than conventional targe ions of a miniature mass spectrometer (drugs and peptides, for example), pressure in the second vacuum stage was tuned to explore the buffer gas pressure effects when analyzing protein ions. The system was pumped by the combination of a tunable turbo pump (70 L/s, KYKY Technology Co. LTD, China) and a diaphragm pump (100 L min^{-1}, Scroll Tech Inc., China), which maintained a pressure of ~4.5 Torr in the first vacuum stage and ~2–16 mTorr in the second vacuum stage. No additional buffer gas was introduced in the system, and air would serve as the buffer gas.

With increased background pressures, the conventional electron multiplier (EM) may no longer be applicable. Therefore, two types of ion detection methods/devices, EM and Faraday detector, were tested and compared. When using an EM (model 2500, Detector Technology Inc., Palmer, MA, USA), a −1.1 kV voltage was applied on the EM, and a −4 kV voltage was applied on the dynodes for positive ion detections. Alternatively, a homemade Faraday detector with a bandwidth of 430 Hz and a gain of 10^{11} V A^{-1} was placed next to the LIT for ion detection. A Faraday detector is charge sensitive, which also does not require working in a vacuum environment. Details about this Faraday detector can be found in our previous publication [58].

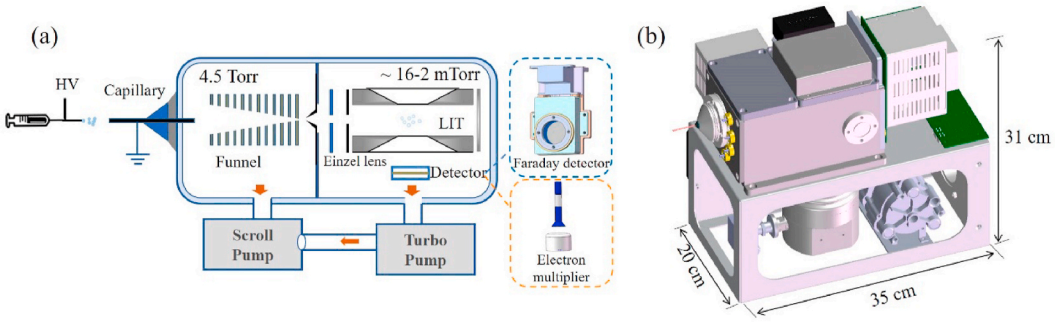

Fig. 1. (a) Structure diagram of the miniature protein mass spectrometer. (b) 3D component assembly of the system.

3. Results and discussion

A LIT with reduced field radius could effectively extend mass range of the instrument. However, as discussed in our previous theoretical work, higher buffer gas pressures would benefit high molecular weight ion analysis [59]. Ion-neutral collisions are important in the operation of an ion trap, which help cooling ions during the ion injection, cooling and ejection processes. Furthermore, for heavier ions, charge sensitive ion detection method may also improve the ion detection sensitivity over velocity sensitive ion detection method [50,60]. Therefore, the instrument was first characterized and optimized in terms of elevated buffer gas pressures and these two detection methods.

3.1. Mass resolution. As a critical parameter, mass resolution was first characterized and optimized by tuning the buffer gas pressure. During the mass selective ion ejection process, it has been found in previous literatures that an optimized buffer gas pressure exists for a fixed mass scan rate (or the sweep rate, details could be found in the Supporting Information) [59,61]. Around this optimized buffer gas pressure, a best mass resolution could be achieved for each type of ions. Conventionally, an ion trap based mass spectrometer was applied for the analysis of small ions typically below 2000 Th, and the ion trap was placed in its optimized pressure range of 1–0.1 mTorr. Our previous theoretical and simulation study has suggested that this optimized buffer gas pressure would be much higher for protein ions [59]. Therefore, pressure in the second vacuum stage of our instrument was gradually tuned in this study, and the peak widths of ions with increased molecular weights were investigated.

The mass analyses of three protein molecules with large molecular

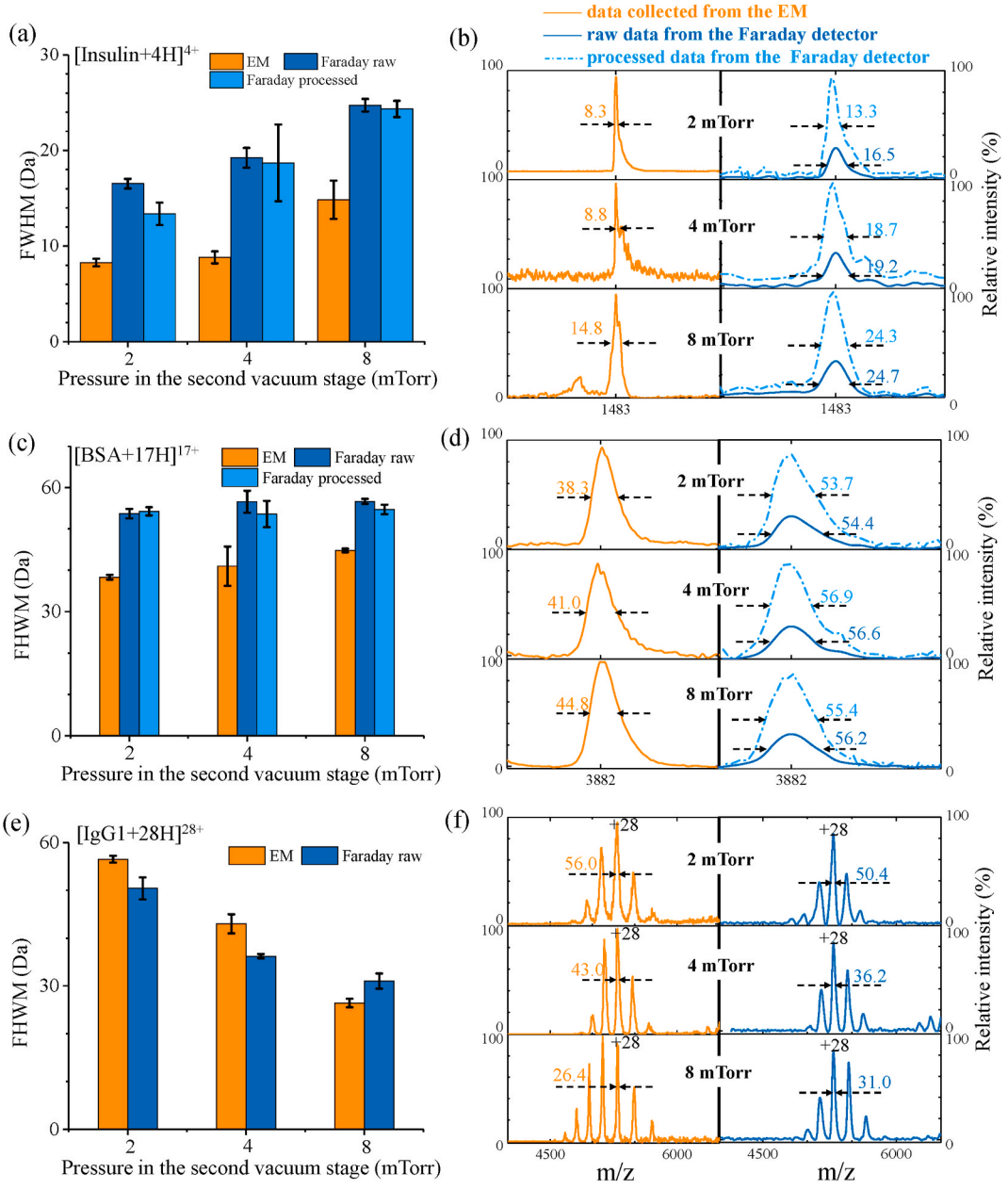

Fig. 2. Mass resolution characterization of the protein mass spectrometer at different pressures. (a) The peak width of insulin 4+ ions (10 μg mL^{-1}) at different pressures. (b) Typical mass spectra of insulin 4+ ions at different pressures. (c) The peak width of BSA 17+ ions (100 μg mL^{-1}) at different pressures. (d) Typical mass spectra of BSA 17+ ions at different pressures. (e) The peak width of IgG1 28+ ions (10 mg mL^{-1}) at different pressures. (f) Typical mass spectra of IgG1 at different pressures. Orange line: mass spectra collected by the EM. Dark blue lines: mass spectra collected by the Faraday detector. Light blue dash dot lines: reconstructed mass spectra. (For interpretation of the references to colour in this figure legend, the reader is referred to the Web version of this article.)

weight differences were carried out at different background pressures, including insulin, BSA and IgG1 (from Trastuzumab). In this experiment, both EM and Faraday detection methods were tested. Fig. 2a plots the peak widths (FWHM, finite width at half maximum) of insulin ions possessing four charges, and Fig. 2b shows the typical mass spectra collected at each working pressure. Results from both EM and Faraday detectors show that broader mass peaks were obtained at higher buffer gas pressures, which is consistent with the theoretical predictions as shown in Fig. S2 and Table S1 in the Supporting Information. Basically, the optimum background pressure for this small protein ion is around 4.5 mTorr. Since pressure inside the LIT is about 2–3 times higher than that in the second vacuum stage [62], the 2–8 mTorr pressure in the second vacuum stage would make the buffer gas pressure higher than the optimum working pressure. It should be noticed that the dipolar resonance excitation AC voltage has been optimized for all pressure cases, which rules out the influence from AC excitation voltage. Furthermore, it should be noticed that the mass peaks collected from the Faraday detector are wider than those from the EM. This is due to the fact that the Faraday detection circuit has a bandwidth of 430 Hz, which is narrower than the bandwidth of the incoming insulin ion signal. In other words, the "sharp" insulin peaks (peak width ~8–15 Th, corresponding to a signal bandwidth ~1218–2285 Hz) were modulated and broadened by the Faraday detection circuit. Therefore, the post data processing method introduced in our earlier work [58] could be applied to reconstruct insulin peaks and neutralize this detector induced broaden effect (light blue bars and lines in Fig. 2a and b).

Nevertheless, larger protein ions would prefer higher buffer gas pressures, and very little or no broadening effects could be observed when using the Faraday detector. As plotted in Fig. 2c and d, the peak widths of BSA (17+) ions have little changes over the pressure range 2–8 mTorr, and narrower mass peaks were actually observed for IgG1 ions with increased pressures (Fig. 2e and f). As molecular weight of an ion increases, the energy exchange during each ion-neutral collision decreases, and fewer cooling effects were acted on the heavy ion. As a result, either higher buffer gas pressure or using heavier buffer gas molecules is required to reach the optimum working condition. Theoretical calculations in Fig. S2 and Table S1 also suggest that 19.8 and 24.5 mTorr are the optimal pressure when analyzing BSA 17+ and IgG1 28+ ions at the scanning speeds used in experiments. Since the peak widths of BSA and IgG1 ions are wider than those of insulin, the 430 Hz bandwidth of the Faraday detector is wide enough for those mass peaks in most cases. Therefore, no obvious peak width change was observed after applying the post data processing method for BSA ions in Fig. 2c and d. The pressure in the second vacuum chamber was further increased to 16 mTorr, and similar mass resolutions were achieved as those obtained at 8 mTorr (Fig. S3 and S4).

3.1. Sensitivity

Besides mass resolution, instrument sensitivity for protein analyses would also be affected by buffer gas pressure and the detection method used. Fig. 3a and c plot the LODs for angiotensin II and BSA at different background pressures. By increasing the background pressure in the second vacuum stage from 2 to 8 mTorr, detection sensitivity has been improved from 0.5 to 0.1 μg mL^{-1} for angiotensin II and 50 to 10 μg mL^{-1} for BSA, respectively. As the background pressure increases, ion-neutral collisions could better help cooling ions into center of the LIT during both the ion injection and cooling periods. For instance, the dual

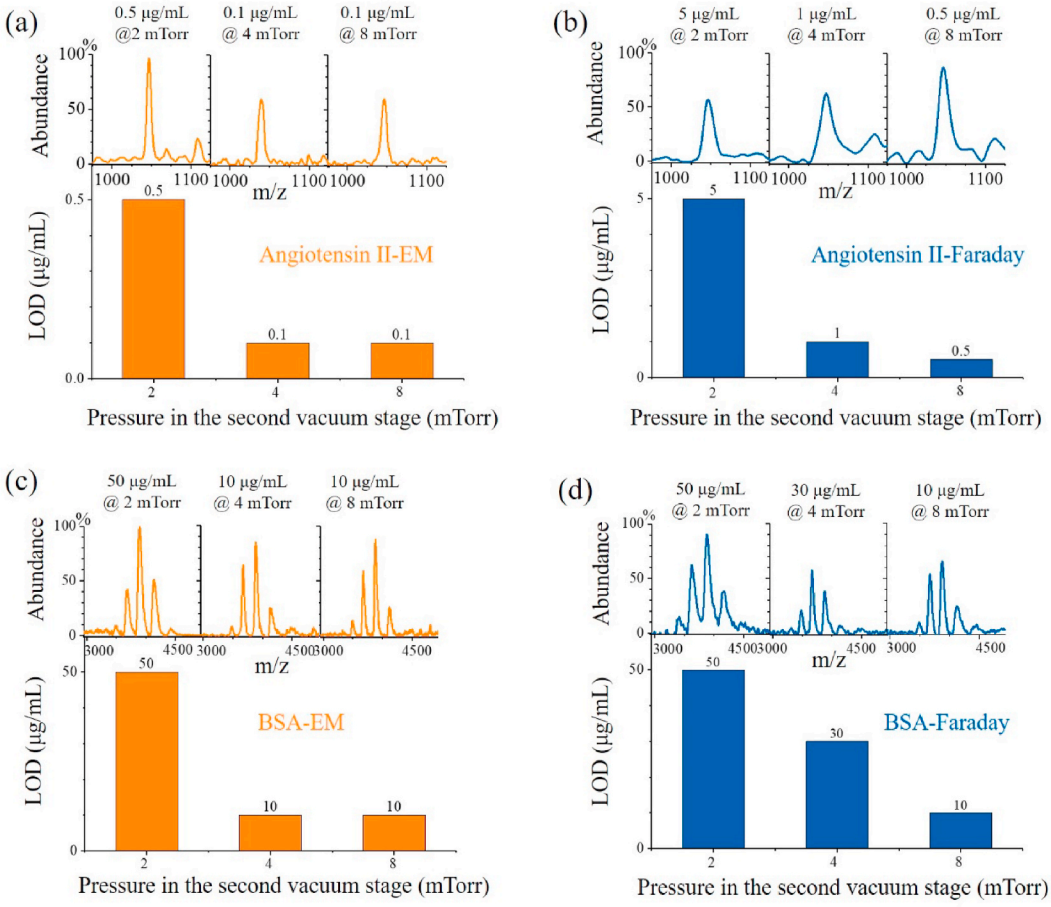

Fig. 3. Instrument sensitivities at different background pressures and using different detection methods. The LOD and mass spectra of angiotensin II using (a) an EM and (b) a Faraday detector. The LOD and mass spectra of BSA using (c) an EM (d) a Faraday detector.

pressure LIT configuration with the first LIT working at elevated pressure (~5 mTorr) has been applied in commercial instruments for improved ion trapping efficiency [35].

On the other hand, Fig. 3b and d plot the LODs of angiotensin II and BSA when using the Faraday detector. Results show that the LODs of angiotensin II are better when an EM is used, which is about 5–10 time better than those of the Faraday detector. This is because small ions could be accelerated to higher velocities during the ion ejection process. As a velocity-sensitive detection, the EM has a larger gain than that of the Faraday detector when detecting small ions [50,60]. However, heavy protein ions would obtain lower velocities than those of light ions during the ion ejection process [41]. Therefore, the gain from the EM would decrease for heavy protein ions. Nevertheless, the Faraday detector is charge sensitive and independent of ion velocities, and its gain is only determined by its amplification circuit. As a result, the LODs achieved using Faraday detection is close or equal to those by using the EM, when analyzing BSA ions (Fig. 3d).

3.2. Signal to noise ratio

Angiotensin II (5 μg mL^{-1}), cytochrome *c* (10 μg mL^{-1}), BSA (100 μg mL^{-1}) and IgG1 (10 mg mL^{-1}) were tested with results shown in Fig. 4. The average value around the characteristic peak is defined as the noise value. The max of the characteristic peak divides the noise value is defined as the signal to noise ratio. When an EM was used (Fig. 4a), the S/N ratio of angiotensin II would increase with respect to pressure; and the S/N ratios of these three protein ions would decrease. In the case when the Faraday detector was used (Fig. 4b), the S/N ratios of all four samples would increase with respect to pressure. Since the Faraday detector has a constant gain, the higher S/N ratios in Fig. 4b would attribute to the better ion cooling effects at higher pressure. The S/N ratios decrease for protein ions in Fig. 4a would be due to the fact that an EM has lower gain for heavy protein ions.

In summary, the use of a Faraday detector and a buffer gas pressure around ~15–25 mTorr (air or nitrogen) within the LIT (~5–12 mTorr within the second vacuum stage) would benefit protein analyses in terms of both mass resolution and sensitivity. In the following protein analyses, the Faraday detector was used, and a pressure of 8 mTorr was maintained in the second vacuum stage of the instrument.

3.3. Analyses of native proteins

After optimization, the instrument was then applied for the analyses of native proteins. To maintain the native structures of proteins, protein samples were dissolved in pure water and then diluted in the ammonium acetate buffer. Samples were then loaded in the nanoESI source through a syringe pump with a flow rate of 1 μL min^{-1}. Since protein ions would possess less ions after ionization under their native conformations, a mass spectrometer with larger upper mass range is required. As stated earlier, an LIT with reduced radius was first used, and frequency of the RF signal was tuned to ~520 KHz. Fig. 5 shows the representative mass spectra of five proteins (from small to large: insulin 10 μg mL^{-1}, cytochrome *c* 10 μg mL^{-1}, lysozyme 30 μg mL^{-1}, BSA 100 μg mL^{-1} and IgG1 from Trastuzumab 10 mg mL^{-1}) collected using the miniature protein mass spectrometer coupled with our home-built Faraday cap detector. It has been shown that the charge state distribution of a protein in an ESI mass spectrum has strong dependence on its conformation in solution [63]. Charge state distributions in Fig. 5 suggest that compact conformations of these proteins were well maintained during the instrument analysis process. Besides molecular weight information, it has been shown that this charge state distribution could reflect protein ion conformation state in their liquid phase [63,64]. Therefore, the combination of *m/z* ratio and charge distribution would provide us information to identify target protein and whether this protein is in its native conformation. Currently, the instrument only has the capability to perform low energy collisional induced dissociation (CID), and it is hard to fragment large protein ions. It would be our further work to try to develop and integrate additional methods for whole protein analyses.

The instrument could also be applied for the analyses of non-native proteins, which could be realized by adjusting the solvent and ESI conditions, for instance. An example of non-native protein analysis could be found in the supporting information (Fig. S5).

4. Conclusions

In this study, a miniature ion trap mass spectrometer was developed and optimized for protein analysis. Mass range of the instrument was extended up to 6500 Th by using a LIT with a field radius of 2.5 mm and lowering the RF frequency to 520 KHz. Since protein ions have relatively large molecular weights, each single ion-neutral collision event has weaker cooling effects on protein ions. Thus, both theory and experiments show that ast buffer gas pressure of ~15–25 mTorr (air) within the LIT is preferred, so that optimized mass resolution and detection sensitivity could be obtained. Furthermore, compared with a conventional EM, the Faraday detection method is more suitable in terms of both its high working pressure and ion velocity independent features. After optimization, instrument capability of performing native MS experiment was demonstrated. Currently, native MS is still a relatively new area for MS instrument development, and some lab-scale instrument could be used for native protein analyses. These instruments

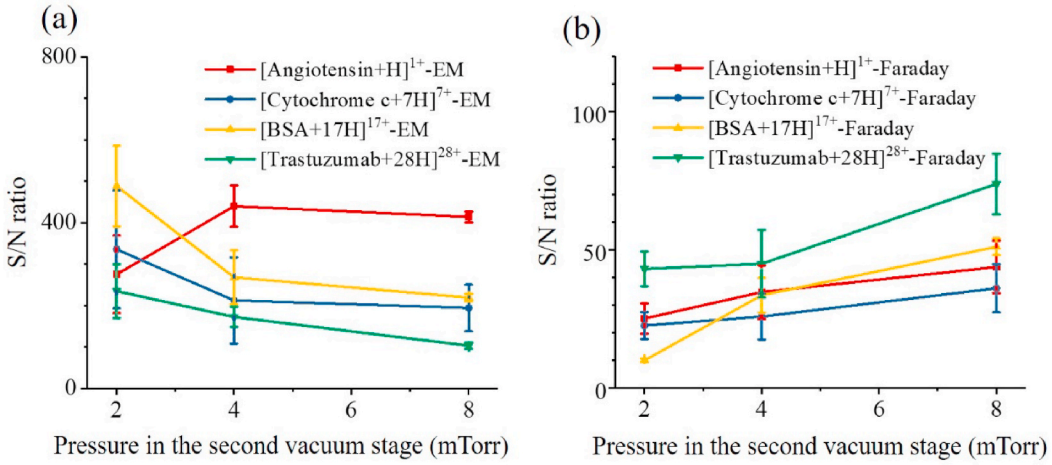

Fig. 4. S/N ratios obtained at different pressures (a) using the EM. (b) using the Faraday detector.

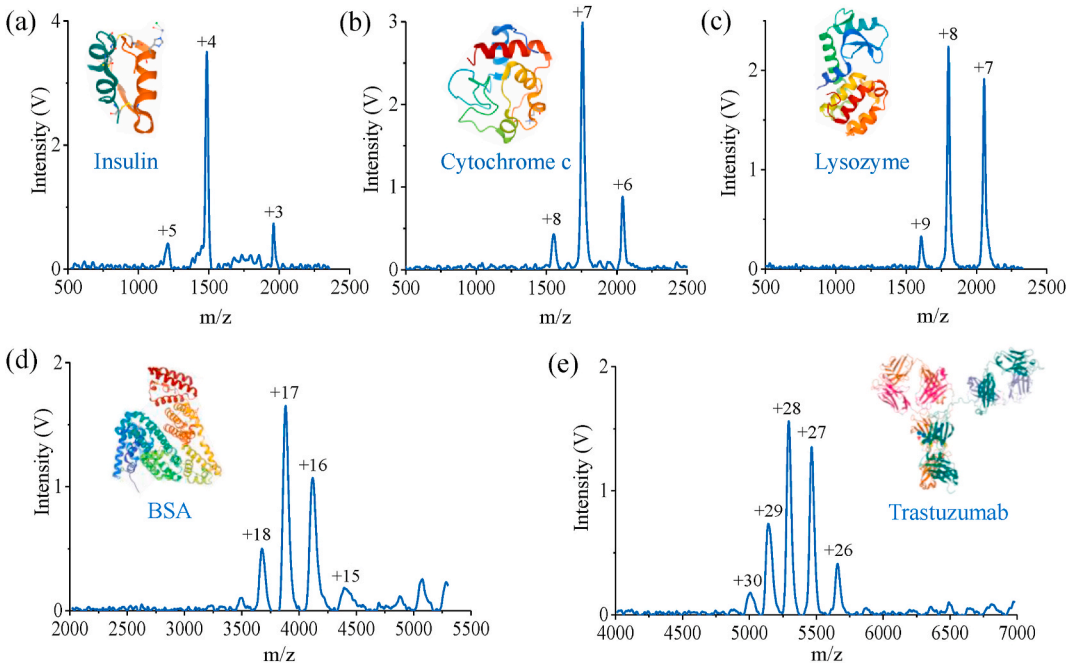

Fig. 5. Mass spectra of native proteins: (a) insulin (b) cytochrome *c* (c) lysozyme (d) BSA (e) IgG1 from Trastuzumab.

typically focus on high resolution, which are expensive and not easy to access. This miniature MS instrument has enough mass resolution to distinguish protein charge state distributions. Thus, as a proof-of-concept demonstration, this current miniature instrument could potentially be used for the rapid identification of target protein and differentiation of its conformation.

Declaration of competing interest

The authors declare that they have no known competing financial interests or personal relationships that could have appeared to influence the work reported in this paper.

Acknowledgements

This work was supported by the National Key Research and Development Program of China (2020YFF01014502) and NNSFC (No. 21922401, 21827810, 61635003).

Appendix A. Supplementary data

Supplementary data to this article can be found online at https://doi.org/10.1016/j.talanta.2021.122580.

Credit author statement

Qian Xu, Methodology, Investigation, Data curation, Validation, Formal analysis, Writing – original draft. Jie Hong, Investigation, Data curation. Siyu Liu, Investigation, Formal analysis, Writing – original draft. Yanbing Zhai, Formal analysis, Writing – review & editing. Wei Xu, Conceptualization, Funding acquisition, Writing – review & editing, Supervision.

References

[1] R.J. Bell, R.T. Short, F.H.W.V. Amerom, R.H. Byrne, Environ. Sci. Technol. 41 (2007) 8123–8128.
[2] H.F. Hemond, Rev. Sci. Instrum. 62 (1991) 1420–1425.
[3] Q.Y. Li, L. Hua, Y. Xie, J. Jiang, H. Li, K. Hou, D. Tian, H.Y. Li, Analyst 144 (2019) 1104–1109.
[4] W. Wang, S. Wang, C. Xu, H. Li, H. Li, Anal. Chem. 91 (2019) 10212–10220.
[5] K. Chingin, H. Chen, G. Gamez, L. Zhu, R. Zenobi, Anal. Chem. 81 (2009) 123–129.
[6] P.S.H. Wong, R.G. Cooks, Anal. Chim. Acta 310 (1995) 387–398.
[7] V. Radulescu, S. Chiliment, E. Oprea, J. Chromatogr. A 1027 (2004) 121–126.
[8] E. Vanhassel, M.E. Bier, Rapid Commun. Mass Spectrom. 21 (2010) 413–420.
[9] X. Zhou, J. Liu, R.G. Cooks, Z. Ouyang, Bioanalysis 6 (2014) 1497–1508.
[10] S.P. Vorce, J.H. Sklerov, K.S. Kalasinsky, J. Anal. Toxicol. 24 (2000) 595–601.
[11] Q. Li, F. Tang, X. Huo, X. Huang, X. Zhang, Anal. Chem. 91 (2019) 8115–8122.
[12] W. Zhang, Y. Ren, Z. Lin, Z. Ouyang, Anal. Chem. 91 (2019) 6986–6990.
[13] J. Ding, H. Gu, S. Yang, M. Li, J. Li, H. Chen, Anal. Chem. 81 (2009) 8632–8638.
[14] K. Biemann, J. Oro, P. Toulmin, L.E. Orgel, A.O. Nier, D.M. Anderson, P. G. Simmonds, D. Flory, A.V. Diaz, D.R. Rushneck, Science 194 (1976) 72–76.
[15] D.T. Snyder, C.J. Pulliam, Z. Ouyang, R.G. Cooks, Anal. Chem. 88 (2015) 2–29.
[16] P.R. Mahaffy, C.R. Webster, M. Cabane, P.G. Conrad, P. Coll, S.K. Atreya, R. Arvey, M. Barciniak, M. Benna, L. Bleacher, SSRv 170 (2012) 401–478.
[17] A.R. Vasavada, J.P. Grotzinger, R.E. Arvidson, F.J. Calef, J.A. Crisp, S. Gupta, J. Hurowitz, N. Mangold, S. Maurice, M.E. Schmidt, J. Geophys. Res. 119 (2014) 1134–1161.
[18] K. Biemann, J. Oro, P. Toulmin, L.E. Orgel, A.O. Nier, D.M. Anderson, P. G. Simmonds, D. Flory, A.V. Diaz, D.R. Rushneck, J. Geophys. Res. 82 (1977) 4641–4658.
[19] W.B. Brinckerhoff, V.T. Pinnick, F.H.W. Van Amerom, R.M. Danell, R.D. Arevalo, M.S. Atanassova, L. Xiang, P.R. Mahaffy, R.J. Cotter, F. Goesmann, IEEE Aerospace Conference, Big Sky, 2013, pp. 1–8. MT (2013.3.2-2013.3.9.
[20] X. Meng, C. Tang, C. Zhang, D. Li, Y. Zhai, J. Am. Soc. Mass Spectrom. 31 (2020) 961–968.
[21] C.J. Pulliam, R.M. Bain, J.S. Wiley, Z. Ouyang, R.G. Cooks, J. Am. Soc. Mass Spectrom. 26 (2015) 224–230.
[22] G. Huang, L. Gao, J. Duncan, J.D. Harper, N.L. Sanders, Z. Ouyang, R.G. Cooks, J. Am. Soc. Mass Spectrom. 21 (2010) 132–135.
[23] S.M. Cristescu, H.A. Gietema, L. Blanchet, C.L.J.J. Kruitwagen, P. Munnik, R.J. Van Klaveren, J.W.J. Lammers, L. Buydens, F.J.M. Harren, P. Zanen, J. Breath Res. 5 (2011), 046009.
[24] A.M. Graichen, R.W. Vachet, J. Am. Soc. Mass Spectrom. 24 (2013) 917–925.
[25] K.H. Blakeman, D.W. Wolfe, C.A. Cavanaugh, J.M. Ramsey, Anal. Chem. 88 (2016) 5378–5384.
[26] S. Ecelberger, T. Cornish, B. Collins, D. Lewis, W. Bryden, JHATD (2004) 25.
[27] W.M. Gilliland, J.M. Ramsey, Anal. Chem. 90 (2018) 13000–13006.
[28] N.G. Davey, E.T. Krogh, C.G. Gill, TrAC Trends Anal. Chem. (Reference Ed.) 30 (2011) 1477–1485.
[29] Huang Dejuan, Luo Liping, Jiang Cuicui, Han Jing, Wang Jiang, J. Agric. Food Chem. 59 (6) (2011) 2148–2156.
[30] Chingin Konstantin, Frankevich Vladimir, R.M. Balabin, Barylyuk Konstantin, Chen Huanwen, Angew. Chem. Int. Ed. (2010).
[31] L. Gao, G. Li, Z. Nie, J. Duncan, Z. Ouyang, R.G. Cooks, Int. J. Mass Spectrom. 283 (2009) 30–34.
[32] Y. Zhai, Y. Feng, Y. Wei, Y. Wang, W. Xu, Analyst 140 (2015) 3406–3414.
[33] T. Jiang, H. Zhang, Y. Tang, Y. Zhai, W. Xu, H. Xu, X. Zhao, D. Li, W. Xu, Anal. Chem. 89 (2017) 5578–5584.
[34] Y. Zhai, X. Zhang, H. Xu, Y. Zheng, T. Yuan, W. Xu, Anal. Chem. 89 (2017) 4177–4183.

[35] X. Liu, X. Wang, J. Bu, X. Zhou, Z. Ouyang, Anal. Chem. 91 (2018) 1391–1398.
[36] J. Fan, P. Lian, M. Li, X. Liu, Z. Ouyang, Anal. Chem. 92 (2020) 2573–2579.
[37] X. Ma, Z. Ouyang, TrAC Trends Anal. Chem. (Reference Ed.) 85 (2016) 10–19.
[38] M. Zhou, C. Lantz, K.A. Brown, Y. Ge, L. Paa-Toli, J.A. Loo, F. Lermyte, Chem. Sci. 11 (2020) 12918–12936.
[39] J.E. Keener, G. Zhang, M.T. Marty, Anal. Chem. 93 (2020) 583–597.
[40] C.H. Chen, Anal. Chim. Acta 624 (2008) 16–36.
[41] W.-P. Peng, S.-W. Chou, A.A. Patil, Analyst 139 (2014) 3507–3523.
[42] L.S. Busenlehner, R.N. Armstrong, Arch. Biochem. Biophys. 433 (2005) 34–46.
[43] A. Baerga-Ortiz, C.A. Hughes, J.G. Mandell, E.A. Komives, Protein Sci. 11 (2002) 1300–1308.
[44] A. Sinz, Mass Spectrom. Rev. 25 (2010) 663–682.
[45] F. Herzog, A. Kahraman, D. Boehringer, R. Mak, A. Bracher, T. Walzthoeni, A. Leitner, M. Beck, F.U. Hartl, N. Ban, Science 337 (2012) 1348–1352.
[46] C. Schmidt, J.A. Macpherson, A.M. Lau, K.W. Tan, F. Fraternali, A. Politis, Anal. Chem. 89 (2017).
[47] S. Carillo, C. Jakes, J. Bones, J. Pharm. Biomed. Anal. 185 (2020) 113218.
[48] B.T. Ruotolo, J.L.P. Benesch, A.M. Sandercock, S.J. Hyung, C.V. Robinson, Nat. Protoc. 3 (2008) 1139–1152.
[49] B. Schindler, A.D. Depland, G. Renois-Predelus, G. Karras, B. Concina, G. Celep, J. Maurelli, V. Loriot, E. Constant, R. Bredy, International Journal for Ion Mobility Spectrometry 20 (2017) pages119–124.
[50] J. Park, Z. Aksamija, H.-C. Shin, H. Kim, R.H. Blick, Nano Lett. 13 (2013) 2698–2703.
[51] X. Huang, J. Jiang, Y. Zhang, L. Zhan, C. Liu, C. Xiong, Z. Nie, Anal. Chem. 91 (2019) 9393–9397.
[52] N.C. Contino, M.F. Jarrold, Int. J. Mass Spectrom. 345 (2013) 153–159.
[53] A.A. Patil, S.-W. Chou, P.-Y. Chang, C.-W. Lee, C.-Y. Cheng, M.-L. Chu, W.-P. Peng, J. Am. Soc. Mass Spectrom. 28 (2016) 1066–1078.
[54] C.-H. Chen, J.-L. Lin, M.-L. Chu, C.-H. Chen, Anal. Chem. 82 (2010) 10125–10128.
[55] L. Wang, F. Xu, C.F. Ding, Anal. Chem. 85 (2013) 1271–1275.
[56] W.-P. Peng, H.-C. Lin, H.-H. Lin, M. Chu, A.L. Yu, H.-C. Chang, C.-H. Chen, Angew. Chem. Int. Ed. 46 (2007) 3865–3869.
[57] J.-L. Lin, M.-L. Chu, C.-H. Chen, Analyst 145 (2020) 3495–3504.
[58] Y. Tang, Q. Xu, D. Li, W. Xu, Analyst 145 (2020) 3892–3898.
[59] C. Hou, Q. Xu, F. Zhang, T. Jiang, W. Xu, J. Mass Spectrom. 54 (2019) 957–965.
[60] J. Park, H. Qin, M. Scalf, R.T. Hilger, M.S. Westphall, L.M. Smith, R.H. Blick, Nano Lett. 11 (2011) 3681–3684.
[61] D.E. Goeringer, W.B. Whitten, J.M. Ramsey, S.A. McLuckey, G.L. Glish, Anal. Chem. 64 (1992) 1434–1439.
[62] X. Huo, X. Zhu, F. Tang, J. Zhang, X. Wang, Anal. Chem. 92 (2020) 3707–3715.
[63] H. Wu, R. Zhang, W. Zhang, J. Hong, Y. Xiang, W. Xu, Chem. Sci. 11 (2020) 4758–4765.
[64] W. Zhang, H. Wu, R. Zhang, X. Fang, W. Xu, Chem. Sci. 10 (2019) 7779–7787.